Image Deblurring with Blur Kernel Estimation in RGB Channels

Xianqiu Xu, Hongqing Liu and Yong Li
Chongqing Key Lab of Mobile Communications Technology
Chongqing University of Posts and Telecommunications
Chongqing, China
hongqingliu@outlook.com

Yi Zhou
School of Communication and Information Engineering
Chongqing University of Posts and Telecommunications
Chongqing, China

***Abstract*—Image deblurring aims to recover the clear image from the damaged image. The most existing blind image deblurring approaches only consider estimating the blur kernel in the gray domain. In fact, for the color image produced by the digital camera, the blur effects for each color channel are usually different. This paper proposes an new approach to acquire more precise blur kernels to reconstruct image by estimating blur kernels through RGB channels independently instead of just using the gray domain. The numerical results demonstrate that proposed approach can achieve better performance compared with other state of the art methods.**

***Index Terms*—Image deblurring, kernel estimation, RGB channels**

I. Introduction

Image quality is always affected by surrounding and outside conditions in the process of acquiring. The image blurring effects caused by camera shake and out-of-focus become one of the most common reasons for poor image quality. With the popularity of handheld cameras, an effective approach that removes motion blur from a captured image is desired for digital image. There are many methods that have been studied in the past two decades, whose purpose is to reconstruct the clear image from the observed degraded image. The existing methods are roughly classified into two categories: blind image deblurring that jointly estimates the blur kernel and the clear image, and non-blind image deblurring that only needs to estimate the clear image using the known kernel. It is well documented that blind image deblurring is an ill-posed problem due to the loss of information on both the images and the blurring process. And the main factor of the blind image deblurring is to precisely estimate the blur kernel [1]. Over the past decade, many studies have been devoted to improve the accuracy of blur kernel estimation. Fergus et al. [2] used a mixture of Gaussian to match the heavy-tailed natural image prior and employed a variational Bayesian framework to estimate the blur kernel. Shan et al. [3] introduced an alternating-minimization method for estimating both blur kernel and the latent image. However, the computational complexity of this approach is high. In [4], Levin et al. used the MAP framework for blur kernel estimation alone rather than a MAP estimation of both the kernel and image, which achieved better performance. These blind image deblurring algorithms only consider estimating the blur kernel in the gray domain, even for the color images. In fact, a color image produced by digital camera can be regarded as a superposition of three color components of the graph, which is red, green and blue, and the blur effects for each color channel are usually different. Ignoring the discrepancy of blur kernels in different color channels usually produces the reconstructed image with annoying errors, e.g., the ringing artifacts.

In this work, an approach to estimate the blur kernels in different channels is developed, and then with the estimated kernels, the image is reconstructed. The blur kernel is first estimated by predicting image salient edges and using Gaussian prior in a multi-scale setting, through three color channels independently instead of just the gray domain. With acquired blur kernel in each color channel, the image is recovered using a robust image deblurring method that explicitly considers errors in the blur kernel estimation and then solved by the accelerated proximal gradient (APG) [5], [6] method. The results demonstrate that the deblurring process is achieved with better performance by considering the difference of blur kernel in each color channel.

II. Problem formulation

Mathematically, the image blurring process can be formulated as the convolution of a clear image with a blur point-spread-function (a.k.a. kernel) plus noise, given by

$$g = h * f + n, \tag{1}$$

where $*$ denotes the discrete convolution operation, h, f, and g denote the blur kernel, the clear image, the observed blurred image, respectively, and n is the noise. The goal of image deblur is to reconstruct the clean image f from the degraded image g.

Let vector $\mathbf{g} = \left[\mathbf{g}_r^{\mathrm{T}}, \mathbf{g}_g^{\mathrm{T}}, \mathbf{g}_b^{\mathrm{T}}\right]^{\mathrm{T}}$ be the blurred color image, where the $\mathbf{g}_r$, $\mathbf{g}_g$ and $\mathbf{g}_b$ are the blurred images of the red, green and blue channels (RGB channel), and the superscript $\mathbf{T}$ is the matrix transpose. Similarly, the clean image can be decomposed with three vectors as $\mathbf{f} = \left[\mathbf{f}_r^{\mathrm{T}}, \mathbf{f}_g^{\mathrm{T}}, \mathbf{f}_b^{\mathrm{T}}\right]^{\mathrm{T}}$, where $\mathbf{f}_r$, $\mathbf{f}_g$ and $\mathbf{f}_b$ are images of RGB channel. The (1) can be now expressed in a matrix-vector form as

$$\mathbf{g} = \mathbf{H}\mathbf{f} + \mathbf{n}, \tag{2}$$

978-1-5090-4165-7/16/$31.00 ©2016 IEEE

where $\mathbf{n}=\left[\mathbf{n}_r^{\mathrm{T}},\mathbf{n}_g^{\mathrm{T}},\mathbf{n}_b^{\mathrm{T}}\right]^{\mathrm{T}}$ is the additive noise vector, and $\mathbf{H}$ is the blur matrix that is a diagonal block matrix, given by

$$\mathbf{H} = \begin{bmatrix} \mathbf{H}_r & 0 & 0 \\ 0 & \mathbf{H}_g & 0 \\ 0 & 0 & \mathbf{H}_b \end{bmatrix}, \tag{3}$$

where $\mathbf{H}_r$,$\mathbf{H}_g$ and $\mathbf{H}_b$ are circular matrices which represent the point spread functions of blur in each color channel. With (2), three different blur matrices can be extracted instead of just one blur kernel in the gray domain, and it is hoped that the better image reconstruction performance can be obtained.

III. Image reconstruction with kernel estimation in RGB channels

A. Kernel estimation in RGB channels

Edge features of the image can be easily detected even though some other structures are weakened. Therefore, we predict the image edge from the observed blurred image using this prior knowledge. Generally speaking, the observed blurred image is usually corrupted by the noise, which produces the inaccurate estimated blur kernel and the reconstructed image with badly ringing artifacts. To reduce the noise interference, Gaussian filtering as the pre-smooth operation is utilized, and then the shock filter is employed to construct significant image edges, given by

$$\partial\mathbf{f}/\partial\mathbf{t} = -\mathrm{sign}(\triangle\mathbf{f})\|\nabla\mathbf{f}\|, \qquad \mathbf{f}_0 = \mathbf{G}_\sigma * \mathbf{f}_{input} \tag{4}$$

where $\nabla\mathbf{f}$ and $\triangle\mathbf{f}$ are the first- and second- order spatial derivatives, respectively, $\mathbf{f}_0$ and $\mathbf{f}_{input}$ refers to the Gaussian smoothed input image and original input image, $\mathbf{G}_\sigma$ denotes the Gaussian filter, $*$ is the discrete convolution operation, and $\mathbf{f}_0$ is used as an initial input for each iteration.

Shock filter will enhance not only the image edges but also the noise. Therefore, the non-significant edge information will be easily confused by the noise, which causes interference of the blur kernel estimation, if not handled. If the scale of blur kernel is bigger than that of the blur kernel, the edge information could damage kernel estimation as well. Therefore, we only select the significant edges to estimate the blur kernel. We transform the image gradients from Cartesian coordinates to polar coordinates, and then select the part of the large gradients. The gradient threshold t is determined based on the size of image and blur kernel, given by

$$t = \max(\sqrt{\mathbf{p}_i\mathbf{p}_k}/15, 10), \tag{5}$$

where $\mathbf{p}_i$ and $\mathbf{p}_k$ represent the total number of pixels of the image and the blur kernel, respectively.

There is also a similar relationship for sharp edges of clear image and blur image in terms of (2). That is

$$\nabla\mathbf{g} = \mathbf{H} * \nabla\mathbf{f} + \mathbf{n}, \tag{6}$$

where $\nabla\mathbf{f}$ and $\nabla\mathbf{g}$ denote the clear image edges and blur image edges, respectively. To estimate the blur kernel, the cost

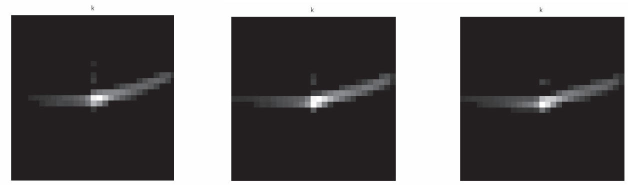

(a) r-kernel (b) g-kernel (c) b-kernel

Fig. 1. Different blur kernels estimation in RGB channels

function is defined by

$$\hat{\mathbf{H}} = \arg\min_{\mathbf{H}} \|\nabla\mathbf{f}^s * \mathbf{H} - \nabla\mathbf{g}\|^2 + \gamma\|\mathbf{H}\|^2, \tag{7}$$

where $\nabla\mathbf{f}^s$ refers to the significant edges information of clear image, and γ is a regularization constant. According to Parseval's theorem, we perform FFTs on all variables and set the derivative with respect to $\mathbf{H}$ to zero. The estimate is obtained by

$$\hat{\mathbf{H}} = \mathbf{F}^{-1}\left(\frac{\overline{\mathbf{F}(\partial_x\mathbf{f}^s)}\mathbf{F}(\partial_x\mathbf{g}) + \overline{\mathbf{F}(\partial_y\mathbf{f}^s)}\mathbf{F}(\partial_y\mathbf{g})}{\overline{\mathbf{F}(\partial_x\mathbf{f}^s)}\mathbf{F}(\partial_x\mathbf{f}^s) + \overline{\mathbf{F}(\partial_y\mathbf{f}^s)}\mathbf{F}(\partial_y\mathbf{f}^s)}\right), \tag{8}$$

where $\mathbf{F}(\cdot)$ and $\mathbf{F}^{-1}(\cdot)$ denote the FFT and inverse FFT respectively, and $\overline{\mathbf{F}(\cdot)}$ is the complex conjugate operator.

Some prior knowledge about kernel can be utilized as well to postprocess the kernel estimation. Generally, the element of blur kernel are non-negative and added up to 1. In this paper, we only select the significant edge information by removing some negative elements to estimate the blur kernel and then normalize the blur kernel.

Using the predicted sharp edge gradient $\nabla\mathbf{f}^s$, we can cursorily recover the blur image by using the following objective function

$$\hat{\mathbf{f}} = \arg\min_{\mathbf{f}} \|\mathbf{f} * \hat{\mathbf{H}} - \mathbf{g}\|^2 + \lambda\|\nabla\mathbf{f} - \nabla\mathbf{f}^s\|^2 \tag{9}$$

By using the FFT and IFFT developed in (7), the closed-form solution for the estimation of the clean image is given by

$$\hat{\mathbf{f}} = \mathbf{F}^{-1}\left(\frac{\overline{\mathbf{F}(\hat{\mathbf{H}})}\mathbf{F}(\mathbf{g}) + \lambda(\overline{\mathbf{F}(\partial_x)}\mathbf{F}(\mathbf{f}_x^s) + \overline{\mathbf{F}(\partial_y)}\mathbf{F}(\mathbf{f}_y^s))}{\overline{\mathbf{F}(\hat{\mathbf{H}})}\mathbf{F}(\hat{\mathbf{H}}) + \lambda(\overline{\mathbf{F}(\partial_x)}\mathbf{F}(\partial_x) + \overline{\mathbf{F}(\partial_y)}\mathbf{F}(\partial_y))}\right). \tag{10}$$

To clearly see this point, blur kernel estimations from a blur image in RGB channels are provided in Figure 1. It is observed that although the main structure is roughly similar, there are still some differences both in the details of edge structure and numerical distribution, suggesting that using three kernels to reconstruct the image may produce better performance.

B. Robust image recovery with estimated blur kernels

No matter how precise the blur kernel estimation is, there will always be errors in the estimation. Ignoring the estimation error will inevitably lead to the performance degradation in the recovered image. In other words, the image recovery method in (10) cannot produce satisfactory performance. Therefore, to consider the estimation error in the kernel, the image recovery model is expressed as follows

$$\mathbf{g} = \mathbf{H}\mathbf{f} + \mathbf{n} = (\hat{\mathbf{H}} - \mathbf{u})\mathbf{f} + \mathbf{n}, \tag{11}$$

where $\mathbf{u}$ is the uncertainty in the matrix $\mathbf{H}$. Performing simple manipulations on (11) yields

$$\mathbf{g} = (\hat{\mathbf{H}} - \mathbf{u})\mathbf{f} + \mathbf{n} = \hat{\mathbf{H}}\mathbf{f} + \mathbf{n} - \mathbf{u}\mathbf{f}. \tag{12}$$

Usually, the error matrix $\mathbf{u}$ is difficult to estimate because of the uncertain blurring process. However, the residual $\mathbf{uf}$ tend to be sparse in the spatial domain, which means that it can be compensated well by using this prior. This is also the so-called error-in-variable (EIV) model in [7]. The error $\mathbf{u}$ could be explicitly removed from the EIV in (12) through estimating both the clear image $\mathbf{f}$ and the residual $\mathbf{uf}$. Also taking the ringing artifacts into consideration, the clear image $\mathbf{f}$ can be recovered via solving the following minimization model in the presence of model error $\mathbf{u}$

$$\begin{aligned}\{\hat{\mathbf{c}}, \hat{\mathbf{r}}, \hat{\mathbf{e}}\} = \arg\min_{\mathbf{c},\mathbf{r},\mathbf{e}} &\Phi(\mathbf{c}, \mathbf{r}, \mathbf{e}) \\ &+ \lambda_1\|\mathbf{c}\|_1 + \lambda_2\|\mathbf{r}\|_1 + \lambda_3\|\mathbf{e}\|_1,\end{aligned} \tag{13}$$

with

$$\begin{aligned}\Phi(\mathbf{c}, \mathbf{r}, \mathbf{e}) = &\frac{1}{2}\|[\hat{\mathbf{H}}(\mathbf{W}^{\mathrm{T}}\mathbf{c} + \mathbf{C}^{\mathrm{T}}\mathbf{r})]_{\Omega} + \mathbf{e} - \mathbf{g}\|_2^2 \\ &+ \kappa\|(\mathbf{I}_m - \mathbf{W}\mathbf{W}^{\mathrm{T}}\mathbf{c})\|_2^2,\end{aligned} \tag{14}$$

where $\mathbf{W}$ is the framelet transform [8], [9] in which the image has a sparse representation, κ and λ are regularization parameters, $\mathbf{I}_m$ denotes the identity matrix, $\mathbf{C}$ denotes the DCT operator, and $\mathbf{c}$, $\mathbf{r}$ and $\mathbf{e}$ represent the wavelet frame coefficients of the clear image, the DCT coefficients of ringing artifacts and the residual $\mathbf{uf}$, respectively, Ω denotes the set of all pixels inside the generation of the image boundary, which means image only work on the region of pixels inside Ω. It makes the deblurring process reliable when the blurring is significant because of avoiding extrapolating the pixel value outside of the boundary. After $\hat{\mathbf{c}}$ is the estimated, the reconstructed image is synthesized via the transform $\hat{\mathbf{f}} = \mathbf{W}^{\mathrm{T}}\hat{\mathbf{c}}$.

The minimization model in (13) is a convex and ℓ_1-norm related minimization problem. The APG method is chosen as the numerical solver for the image recovery due to fast convergence rate. The APG algorithm is offered for solving the following convex optimization problem

$$\min_{x \in R^n} F(x) + G(x), \tag{15}$$

where $F(\cdot)$ is convex, continuously differentiable and its gradient ∇F is Lipschitz continuous on $\mathbf{R}^n$, and $G(\cdot)$ is convex but not necessarily differentiable. In order to apply the ARG algorithm, the optimization problem in (13) is rewritten as

$$\begin{aligned}\{\hat{\mathbf{c}}, \hat{\mathbf{r}}, \hat{\mathbf{e}}\} &= \arg\min_{\mathbf{c},\mathbf{r},\mathbf{e}} \Phi(\mathbf{c}, \mathbf{r}, \mathbf{e}) + \lambda_1\|\mathbf{c}\|_1 + \lambda_2\|\mathbf{r}\|_1 + \lambda_3\|\mathbf{e}\|_1 \\ &= F(\mathbf{c}, \mathbf{r}, \mathbf{e}) + G(\mathbf{c}, \mathbf{r}, \mathbf{e}),\end{aligned} \tag{16}$$

where

$$\begin{aligned}F(\mathbf{c}, \mathbf{r}, \mathbf{e}) &= \frac{1}{2}\|[\hat{\mathbf{H}}(\mathbf{W}^{\mathrm{T}}\mathbf{c} + \mathbf{C}^{\mathrm{T}}\mathbf{r})]_{\Omega} + \mathbf{e} - \mathbf{g}\|_2^2 \\ &\quad + \kappa\|(\mathbf{I}_m - \mathbf{W}\mathbf{W}^{\mathrm{T}}\mathbf{c})\|_2^2 \\ G(\mathbf{c}, \mathbf{r}, \mathbf{e}) &= \lambda_1\|\mathbf{c}\|_1 + \lambda_2\|\mathbf{r}\|_1 + \lambda_3\|\mathbf{e}\|_1.\end{aligned} \tag{17}$$

In $G(\mathbf{c}, \mathbf{r}, \mathbf{e})$, it is a ℓ_1-norm minimization problem, and its solution can be obtained by the component-wise soft-thresholding operator, given by

$$\mathbf{T}_{\lambda}(a) = \begin{cases} a - \lambda, & a > \lambda \\ 0, & |a| < \lambda \\ a + \lambda, & a < -\lambda. \end{cases} \tag{18}$$

IV. Numerical Studies

In this section, simulations are conducted to confirm the performance of our proposed approach for blur images. In all the experiments, the parameter $\gamma = 10$, $\lambda = 2e^{-3}$, λ_2, λ_3 as $5\lambda_1$ and $2\lambda_1$ are set, respectively, and the value of λ_1 is chosen according to the image noise level. The peak-signal-to-noise ratio (PSNR) as the performance measure is employed, given by

$$\mathrm{PSNR} = -10\log_{10}[\frac{1}{255^2 \times N}\sum_{i=1}^{N}(f_i - \hat{f}_i)^2] \tag{19}$$

where N is the size of the image, f_i is the intensity value of the clear image, and $\hat{f}_i$ denotes the intensity value of recovered image.

(a) (b)

(c) PSNR=28.0932 (d) PSNR=29.2327

Fig. 2. Results of deblurring from image "lena". (a) the truth image. (b) the input blur image blurred by Gaussian blur with $\sigma = 3$. (c) deblurring by kernel estimation with gray domain,(d) deblurring by kernel estimation in RGB channels.

In the first experiment, the synthesized degraded images were used to demonstrate the performance of the proposed method. The test images are blurred by the given blur kernel and then corrupted by addition Gaussian noise. The results are provided in Figure 2 and Figure 3, where the Gaussian blur kernel with $\sigma = 3$ and linear motion blur kernel with length 10 pixels and $10°$ orientation are used to generate the blurred image respectively. It is seen that by considering the differences of blur kernel in each color channel, the reconstructed image is clear and the PSNR is higher than that of just using blur kernel estimation in the gray domain.

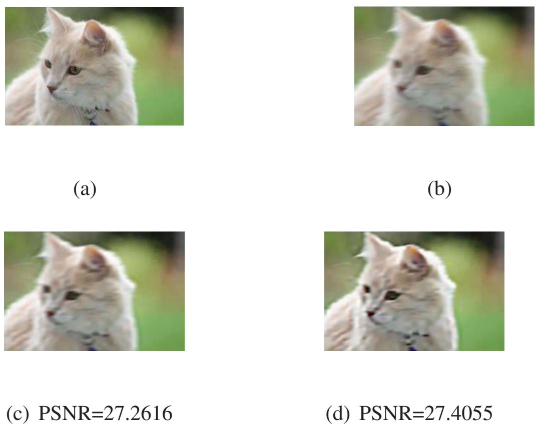

Fig. 3. Results of deblurring from image "cat". (a) the truth image, (b) the input blur image blurred by linear motion blur with length 10 pixels and 10° orientation. (c) deblurring by kernel estimation with gray domain,(d) deblurring by kernel estimation in RGB channels.

In the second experiment, the proposed method is tested on real blur images and the results are compared with only considering estimating blur kernel with gray domain as well. Due to the lack of the real clear image information, we only compared simulation results from the perspective of the visual effects. From the results, the restored images are clearer than that of using gray domain estimation, which means that ignoring blur kernel's differences of different color channels indeed degrades the reconstruction performance.

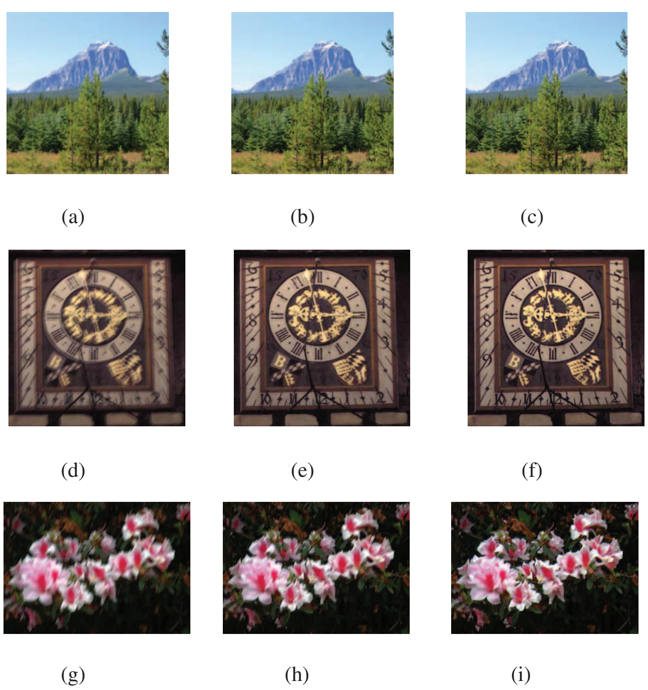

Fig. 4. Results of deblurring from true blur images. (a), (d), (g) the input blur image (b), (e), (h) deblurring by kernel estimation with gray domain, (c), (f), (i) deblurring by kernel estimation in RGB channels.

V. Conclusion

To better recover the clear image, in this work, the blur differences are employed in the different color channels in the kernel estimation. To consider the error in the kernel estimation, a robust image reconstruction approach is utilized that explicitly removes the error in the blur kernel, and then the resulting optimization problem is solved by the APG method. The numerical examples demonstrate that the deblurring results are improved by utilizing the difference of blur kernel in each color channel compared to just using the single blur kernel in the gray domain. Our future work will focus on optimizing the blur kernel estimation methods to recover the clear images with large blurs.

Acknowledgment

The authors would like to thank Dr. Hui Ji, National University of Singapore for his image deblur code. This work was jointly supported by Foundation and Advanced research projects of Chongqing Municipal Science and Technology Commission under Grants cstc2014jcyjA40017, cstc2014jcyjA40027 and cstc2015jcyjA40027, by the National Natural Science Foundation of China under Grants 61401050 and 61501072, by the Ministry of Education Scientific Research Foundation for Returned Overseas Chinese F201405.

References

[1] L. Xu and J. Jia, "Two-phase kernel estimation for robust motion deblurring," *Computer Vision-ECCV*, vol. 4, 2010.
[2] R. Fergus and B. Singh, "Removing camera shake from a single photograph," *ACM Transactions on Graphics*, vol. 25, no. 25, pp. 787–794, 2006.
[3] Q. Shan, J. Jia, and A. Agarwala, "High-quality motion deblurring from a single image," *ACM Transactions on Graphics*, vol. 27, no. 3, pp. 15–19, 2008.
[4] A. Levin, Y. Weiss, F. Durand, and W. T. Freeman, "Understanding and evaluating blind deconvolution algorithms," *IEEE Conference on Computer Vision & Pattern Recognition*, vol. 8, no. 1, pp. 1964–1971, 2009.
[5] A. Beck and M. Teboulle, "A fast iterative shrinkage-thresholding algorithm for linear inverse problems," *SIAM Journal on Imaging Science*, vol. 2, no. 1, pp. 183–202, sep. 2009.
[6] Z. Shen, K. Toh, and S. Yun, "An accelerated proximal gradient algorithm for frame based image restorations via the balanced approch," *SIAM Journal on Imaging Science*, vol. 4, no. 2, pp. 573–596, 2011.
[7] H. Ji and K. Wang, "Robust image deblurring with an inaccurate blur kernel," *IEEE Transactions on Image Processing*, vol. 21, no. 4, pp. 1624–34, 2012.
[8] J. Cai and Z. Shen, "Framelet based deconvolution," *J. Comp. Math.*, vol. 28, no. 3, pp. 289–308, 2010.
[9] J. F. Cai, S. Osher, and Z. Shen, "Linearized bregman iterations for frame-based image deblurring," *SIAM Journal on Imaging Sciences*, vol. 2, no. 1, pp. 226–252, 2010.